

This work was written as part of one of the author's official duties as an Employee of the United States Government and is therefore a work of the United States Government. In accordance with 17 U.S.C. 105, no copyright protection is available for such works under U.S. Law.

Public Domain Mark 1.0

<https://creativecommons.org/publicdomain/mark/1.0/>

Access to this work was provided by the University of Maryland, Baltimore County (UMBC) ScholarWorks@UMBC digital repository on the Maryland Shared Open Access (MD-SOAR) platform.

Please provide feedback

Please support the ScholarWorks@UMBC repository by emailing scholarworks-group@umbc.edu and telling us what having access to this work means to you and why it's important to you. Thank you.

SCALING OF THE ELECTRON DISSIPATION RANGE OF SOLAR WIND TURBULENCE

F. SAHRAOUI¹, S. Y. HUANG², G. BELMONT¹, M. L. GOLDSTEIN³, A. RÉTINO¹, P. ROBERT¹, AND J. DE PATOUL¹

¹ Laboratoire de Physique des Plasmas, CNRS-Ecole Polytechnique-UPMC, Route de Saclay, F-92120 Palaiseau, France; foudad.sahraoui@lpp.polytechnique.fr

² School of Electronics and Information, Wuhan University, Wuhan, China

³ NASA Goddard Space Flight Center, Code 672, Greenbelt, MD 20771, USA

Received 2013 May 2; accepted 2013 July 29; published 2013 October 9

ABSTRACT

Electron scale solar wind (SW) turbulence has attracted great interest in recent years. Considerable evidence exists that the turbulence is not fully dissipated near the proton scale, but continues cascading down to electron scales. However, the scaling of the magnetic energy spectra as well as the nature of the plasma modes involved at those small scales are still not fully determined. Here we survey 10 yr of the *Cluster* STAFF search-coil magnetometer waveforms measured in the SW and perform a statistical study of the magnetic energy spectra in the frequency range [1, 180] Hz. We found that 75% of the analyzed spectra exhibit breakpoints near the electron gyroscale ρ_e , followed by steeper power-law-like spectra. We show that the scaling below the electron breakpoint cannot be determined unambiguously due to instrumental limitations that we discuss in detail. We compare our results to those reported in other studies and discuss their implications for the physical mechanisms involved and for theoretical modeling of energy dissipation in the SW.

Key words: plasmas – solar wind – turbulence

Online-only material: color figures

1. INTRODUCTION

Our understanding of magnetofluid turbulence in astrophysical plasmas depends in large part on the in situ measurement and interpretation of data taken in the near-Earth space plasmas such as the solar wind (SW) or the magnetosheath. This is a direct consequence of the availability of high quality data from many space missions, including *Voyager 1* and 2, *Ulysses*, *ACE*, *Wind*, *Stereo*, and *Cluster*, to name but a few.

While previous data sets have been useful for addressing turbulence at scales larger than the ion gyroscale, typically $\rho_i \sim 100$ km at 1 AU (corresponding to an observed spacecraft frame frequency of $f_{\rho_i} \sim 0.5$ Hz assuming that the Taylor frozen-in-flow approximation holds⁴), i.e., the so-called inertial range, the high time resolution *Cluster* data have opened a new chapter in turbulence studies that focuses on electron scales ($L \sim \rho_e \sim 1$ km, where ρ_e is the electron gyroradius; Sahraoui et al. 2009, 2010a; Kiyani et al. 2009; Alexandrova et al. 2009). These observations have driven intensive research work on electron scale turbulence, both theoretically and numerically (Meyrand & Galtier 2010, 2012; Podesta et al. 2010; Chang et al. 2011; Valentini et al. 2011; Camporeale & Burgess 2011; Howes et al. 2011b; Gary et al. 2012; Sahraoui et al. 2012). Determining the nature and properties (e.g., scaling, anisotropy) of the turbulence at small scales is crucial to understanding the problems of energy dissipation and heating, particle acceleration, and magnetic reconnection in space and astrophysical plasmas (Schekochihin et al. 2009). Analyses of the high time resolution search-coil magnetometer (SCM), which provides waveforms of the magnetic field fluctuations up to 180 Hz, have demonstrated that SW turbulence does cascade below the ion gyroscale ρ_i down to the electron scale ρ_e where dissipation becomes important and the spectra are observed to steepen significantly. However, the

underlying physics is still very controversial, owing to the fact that the available observations are very few and the theoretical and numerical work has only very recently been extended to those small scales (Chang et al. 2011; Camporeale & Burgess 2011; Howes et al. 2011b; Gary et al. 2012; Sahraoui et al. 2012; Meyrand & Galtier 2012).

From an observational point of view, only a handful of observations of SW turbulence exist at electron scales and all do not agree. The first point of controversy is the scaling of the magnetic energy spectra down to and below ρ_e . Sahraoui et al. (2009) first reported a power-law cascade $\sim f^{-2.5}$ down to f_{ρ_e} , where a clear spectral break was observed followed by another power-law-like band that was close to f^{-4} (f_{ρ_e} is the Taylor-shifted electron gyroscale). Sahraoui et al. (2009) emphasized that the fit below f_{ρ_e} should be viewed cautiously because of the limited bandwidth that extended into the electron dissipation range, a limitation imposed by the sensitivity of the SCM (see Section 5 below). Similar power-law-like spectra have been reported in Sahraoui et al. (2010a) and Kiyani et al. (2009). On the other hand, Alexandrova et al. (2009), using STAFF-Spectrum Analyzer (STAFF-SA) data, have reported exponential scaling $\sim \exp(-\sqrt{k\rho_e})$ in the range $k\rho_e \sim [0.1, 1]$. More recently, Alexandrova et al. (2012) proposed a different model and proposed a new scaling $k_{\perp}^{-8/3} \exp(-k_{\perp}\rho_e)$ as a better fit to the data in the range $k\rho_e \sim [0.03, 3]$. We will refer to the above three models as the *double-power-law*, the *exponential*, and the *hybrid*, respectively. In addition to those three models, we introduce below a new one, the *asymptotic-double-power-law*. We show that the exponential model does not provide as good a fit to the data as the double-power-law model. We show, however, that, due to *Cluster* instrumental limitations that we discuss in detail, it may not always be possible to distinguish between the three remaining models, the main difference between them being whether or not a spectral break is seen near ρ_e .

From a theoretical point of view, recent numerical simulations have tried to tackle the problem of cascade and dissipation at

⁴ It is commonly referred to as the Doppler-shifted ion gyroradius, although it is not a very appropriate definition considering that Doppler shift applies to frequencies and not to spatial scales. Here we introduce the terminology of the “Taylor-shifted scale.”

electron scales. Camporeale & Burgess (2011) performed two-dimensional full particle-in-cell (PIC) simulations of decaying electromagnetic fluctuations near and below the electron inertial length d_e . They showed that the magnetic energy spectra steepen from $k_{\perp}^{-2.6}$ to $k_{\perp}^{-5.8}$ with a clear spectral break at $k\rho_e \sim 1$. Three-dimensional PIC simulations of whistler-driven turbulence showed very similar results with less steep spectra, $\sim k_{\perp}^{-4.5}$, at scales $k_{\perp}d_e \gtrsim 1$ (Chang et al. 2011; Gary et al. 2012). Gyrokinetic (GK) simulations of strong kinetic Alfvén wave (KAW) turbulence, which self-consistently contain kinetic damping of the low frequency plasma modes ($\omega \ll \omega_{ci}$) but do not include the cyclotron resonance, showed a clear power-law cascade $k_{\perp}^{-2.8}$ down to $k_{\perp}\rho_e \sim 1$ (Howes et al. 2011b). The GK theory predicts magnetic energy spectra with a scaling $k_{\perp}^{-16/3}$ for the (entropy) cascade below ρ_e (Schekochihin et al. 2009). On the other hand, Meyrand & Galtier (2010) showed that incompressible electron MHD (EMHD) turbulence predicts that the magnetic energy spectra should follow a power law $k^{-11/3}$ at scales smaller than d_e . That steepening was proposed to explain the observed spectra below the electron scale reported in the SW (Sahraoui et al. 2009, 2010a). Although this fluid model is non-dissipative and does not consider any damping of the turbulence via kinetic effects, which are important in the dispersive and the dissipation ranges, it nevertheless has the merit of proving that fully nonlinear dynamics and dispersive effects in EMHD leads to a steepening of the energy spectra near d_e . Thus, all existing theoretical and numerical predictions published so far support the double-power-law model to reproduce the scaling near and below the electron gyroscale or inertial length.

In a recent paper by Howes et al. (2011a), it was pointed out that for $\beta_i \ll 1$ kinetic damping of KAW turbulence becomes strong, which results in a cut-off of the spectra at moderate wavenumber, typically $k_{\perp}\rho_i \sim 10$. This is inconsistent with SW observations (Sahraoui et al. 2009, 2010a; Alexandrova et al. 2009). To overcome the failure of the model to reproduce SW observations, Howes et al. (2011a) suggested that non-local effects due to large scale shear flows play a role in sustaining the energy cascade down to smaller scales. When such non-local effects are considered, it was indeed shown that the energy cascade in low β_i can reach scales of $k_{\perp}\rho_e \sim 1$, where the spectra curve and show an exponential-like behavior. For $\beta_i \gtrsim 1$ relevant to the SW, both the local and the non-local models give the same power-law scaling of the magnetic energy spectra down to $k_{\perp}\rho_e \sim 1$ (Howes et al. 2011a, 2011b), which may indicate that non-local effects do not play an important role in this case. We will return to this discussion below.

Here, we report a large statistical survey of SW turbulence using the *Cluster* SCM waveforms low-pass filtered at 180 Hz. We focus particularly on the scaling of the magnetic energy spectra up to and above f_{ρ_e} , the frequency corresponding to Taylor-shifting the electron gyroscale, ρ_e . In Section 2, we explain the approach we used to select the *Cluster* data in the SW. We particularly target intervals when the *Cluster* fleet is located in the SW, thus excluding data from the electron and ion foreshock (EFS and IFS, respectively) regions, and when the signal-to-noise ratio (S/N) of the magnetic fluctuations is high. In Section 3, we introduce the fitting models that we use to fit the spectra. In Section 4, we show the main results of the study and discuss them in light of existing theoretical and numerical predictions and earlier work related to the subject. In Section 5, we discuss several caveats that need to be handled carefully in order to avoid any misinterpretation of the observations.

2. DATA SELECTION

In the present study, we surveyed all STAFF-SC burst mode (BM) waveform data measured in the SW by the *Cluster* spacecraft C3 from 2000 to 2011 in the frequency range [1, 180] Hz. The SCM data was calibrated using the continuous calibration method described in P. Robert et al. (2013, in preparation). We used the AMDA data base (<http://cdpp-amda.cesr.fr/DDHTML/index.html>) to select intervals of time when the *Cluster* spacecraft were located in the SW. AMDA provides useful routines to search for data according to desired physical parameters (e.g., high or low SW speeds and plasma β). The list of events is then checked event by event with respect to WHISPER (Décréau et al. 1997) and PEACE (Johnstone et al. 1997) data to remove any interval containing foreshock electrons (see an example of the targeted SW intervals in Figure 3). By removing all data contaminated by foreshock electrons, we aim to unambiguously answer the question as to whether or not the magnetic energy spectra in the free-streaming SW exhibit spectral breaks at electron scales.

Eliminating data from the IFS region or from other boundaries such as interplanetary shocks (IPs) or coronal mass ejections (CMEs) requires using data from the Cluster Ion Spectrometer (CIS; Rème et al. 2001). The free-streaming SW is generally characterized by a beam of ions with an energy around 1–2 KeV. Any enlargement of the beam toward higher energies generally indicates the heating of ions across boundaries such as shocks. The CIS spectrograms, available at the ESA Cluster Active Archive (CAA) Web site (<http://caa.estec.esa.int/caa/home.xml>), allow one to identify the IFSs and IPSs. However, the spectrograms cannot guarantee the absence of any reflected ions from the shock, which can be detected only by a careful analysis of the ion distributions functions (IDFs). In the following, to eliminate the significant EFSs, IFSs, and IPSs, we rely mostly on the examination of the WHISPER, PEACE, and CIS spectrograms. If there is still doubt, we then analyze the corresponding IDFs provided at the CAA to check for reflected energetic ions from the foreshock.⁵ Despite these numerous checks of the data, one still needs to assume that residual reflected ions from the foreshock might still exist in our data and not be observable on the spectrograms or in the analyzed IDFs, but they do not have significant impact on the electron scale physics, which is the main purpose of the present paper. Indeed, such ions, when they exist, would affect ion scales $\sim \rho_i$ rather than electron scales $\sim \rho_e$ through, for instance, ion plasma instabilities that might be generated in the SW plasma.

After obtaining the list of events that survive the different criteria given above, we focus only on intervals where magnetic fluctuations have a high S/N. The S/N (in dB) is defined as a fraction of the measured frequency onboard the spacecraft (Sahraoui et al. 2010b)

$$S/N(f_{sc}) = 10 \log_{10} \left[\frac{\delta B^2(f_{sc})}{\delta B_{sens.}^2(f_{sc})} \right],$$

where δB and $\delta B_{sens.}$ are, the amplitude of the magnetic fluctuation and the level of the sensitivity floor of the *Cluster* SCM at the frequency f_{sc} , respectively. To accomplish this,

⁵ The IDFs given in the ESA/CAA Web site may need a careful post-treatment to obtain clean IDFs in the SW. However, doing such detailed studies of the IDFs is hardly feasible for all our events (C. Mazelle 2012, private communication).

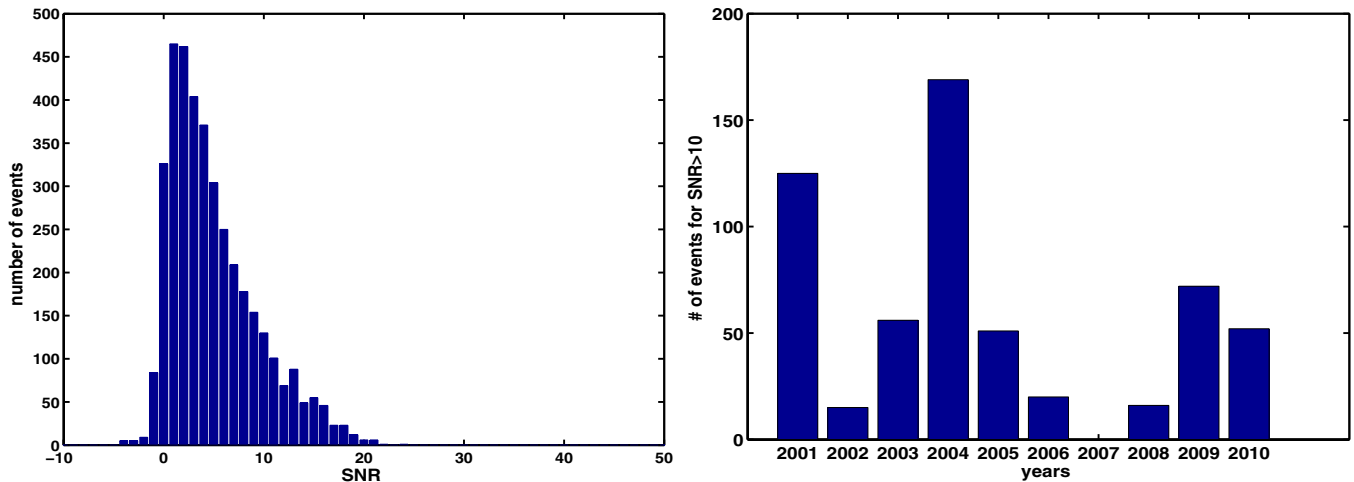


Figure 1. Distribution of the signal-to-noise ratio at $f = 30$ Hz of the B_z magnetic energy spectra (GSE) measured in the free-streaming SW from 2000 to 2011 (left). The distribution of the found spectra with $S/N > 10$ at 30 Hz (15% \sim 610 spectra) over the 10 yr survey (right).

(A color version of this figure is available in the online journal.)

we computed the magnetic energy spectra over approximately 10 s for all intervals and estimated the value of the S/N at the frequency $f_{sc} \simeq 30$ Hz. With a SW speed $V_{sw} \sim 500$ km s $^{-1}$ and an electron gyroradius $\rho_e \sim 1$ km, the frequency $f_{sc} = 30$ Hz roughly corresponds to the scale $k\rho_e \sim 0.4$ using the Taylor assumption. The obtained histogram (Figure 1) shows that at $f_{sc} \simeq 30$ Hz most of the turbulent spectra reach the sensitivity floor of the *Cluster* SCM, which means that those events cannot be used to address the electron scale physics (other histograms of S/N were computed at neighboring frequencies and found to be very similar to the one shown here). To achieve this goal, we need to select intervals with the highest possible S/N . However, as can be seen in Figure 1, the higher the S/N is, the rarer the events are. Here we present only the results for events having $S/N \geq 10$, and only 610 were found. These events represented about 15% of the total events. An “event” refers to a total power spectrum computed over nearly 10 s period of time where the mean magnetic field and the SW plasma parameters do not change significantly. This time duration has been chosen to cover the frequency range $\sim [1, 180]$ Hz. Longer time intervals would be required to study lower frequencies, but that range will not be addressed here.

3. FITTING MODELS

As we discussed above, the theoretical and numerical studies of SW turbulence dissipation at electron scale are very recent. The absence of firm theoretical predictions on this problem and the limitations of the available data make it difficult to draw firm conclusions on the actual processes of dissipation, or even on the actual scaling of the energy spectra at electron scales. To tackle this last question, we propose to test a few fitting models proposed in the literature to determine which one better fits the measured magnetic energy spectra from our statistical study. The fitting models we use are as follows.

1. Double-power-law model

$$P(f) = A_1 f^{-\alpha_1} [1 - H(f - f_b)] + A_2 f^{-\alpha_2} H(f - f_b).$$

2. Exponential model

$$P(f) = A \exp(-a \sqrt{f/f_b}).$$

3. Hybrid model

$$P(f) = A f^{-\alpha_1} \exp(-f/f_b).$$

4. Asymptotic-double-power-law model

$$P(f) = A \frac{f^{-\alpha_1}}{1 + (f/f_b)^2},$$

where $H(f)$ is the Heaviside function and f_b is the frequency of the breakpoint at electron scale. The last model is asymptotically similar to the double-power-law model: for $f \ll f_b$ $P(f) \sim A f^{-\alpha_1}$ and for $f \gg f_b$ $P(f) \sim f^{-\alpha_1-2}$. However, when $f \sim f_b$, this model is very close to the hybrid model and results in a curved spectrum. Note that in the double-power-law model, the break frequency f_b corresponds to the intersection of the two power-law fits and is given by Equation (5) in Alexandrova et al. (2012). Our fitting models are given as functions of the measured frequency onboard the spacecraft. If one assumes that the break frequency corresponds to the electron gyroscale, i.e., $f/f_b \sim k\rho_e$, then one can recover exactly the fitting functions in wavenumber used in Alexandrova et al. (2009, 2012). However, those fitting models explicitly assume that the Taylor frozen-in-flow approximation is valid even at electron scales and, generally, that the \mathbf{k} vectors of the turbulence are parallel to the flow speed (i.e., $\omega_{sc} \sim \mathbf{k} \cdot \mathbf{V} \sim kV$). These are strong assumptions considering that at electron scales whistler-like fluctuations may exist, which might have phase speeds of the order of or larger than the flow speed, and that turbulence wave vectors \mathbf{k} at sub-ion scales were shown to form angles $\sim 40^\circ$ with respect to the mean flow (Sahraoui et al. 2010a). To avoid making any such strong assumptions, we choose to fit our data in the frequency domain as it is measured onboard the spacecraft. When needed, we simply indicate on the plots the approximate location of the electron characteristic scales if the Taylor assumption were valid.

One should stress here that these functions are chosen purely for mathematical reasons and they do not necessarily reflect actual physical mechanisms of dissipation, although there may exist a possible connection between a given scaling with a particular dissipation process. For example, hydrodynamic turbulence is known to yield an exponential dissipation, while

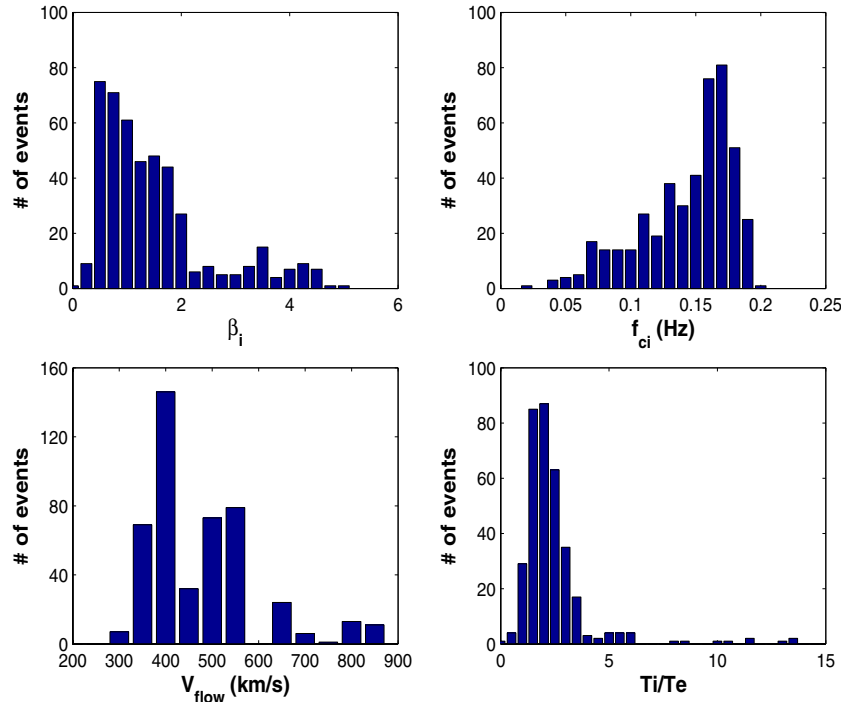


Figure 2. Histograms of different mean SW parameters: β_i , ion cyclotron frequency f_{ci} , the solar wind speed V_{flow} , the ratio of ion to electron temperatures, and the distribution of the events over the 10 yr survey.

(A color version of this figure is available in the online journal.)

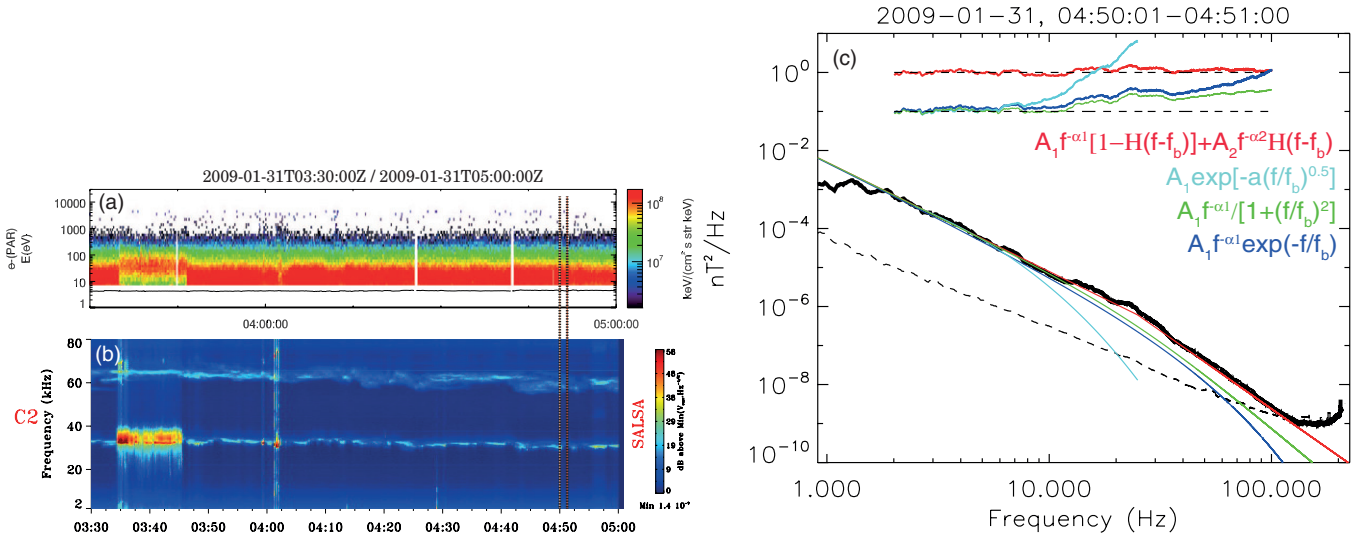


Figure 3. Typical example of the analyzed events: (a) the spectrogram of field-aligned electron energy from PEACE (C1; no data available on C2), (b) is the electric field from WHISPER, showing that the spacecraft is in the free SW from 04h05 to 05h00 (no foreshock electrons), and (c) a magnetic energy spectrum of B measured in the SW by the *Cluster 2*/STAFF-SC instrument (black). The dashed line indicates the estimated (in-flight) sensitivity floor of the instrument. Examples of fitting functions are plotted for comparison ($f_b \sim 25$ Hz, $\alpha_1 = 2.6$, $\alpha_2 = 4.2$, and $a = 15$): double-power-law (red), asymptotic-double-power-law (green), hybrid (blue), and exponential (cyan). The horizontal curves are compensated spectra $B^2(f)/P(f)$, where $P(f)$ is the corresponding fitting function.

(A color version of this figure is available in the online journal.)

asymptotic-double-power-law models have been reported in fusion plasma turbulence where the finite Larmor effects play a key role (Hasegawa et al. 1978; Gurcan et al. 2009).

4. RESULTS

For the obtained list of events, we computed the histograms of the corresponding mean plasma parameters, which are given in Figure 2. These parameters are typical of the SW conditions, with most of the events having $T_i > T_e$ and $\beta_i \geq 1$.

An example of the studied events in the free-streaming SW is shown in Figure 3. The magnetic energy spectrum in Figure 3(c) shows that turbulence cascades below the ion scale and reaches the electron gyroscale where a clear break is apparent, in agreement with earlier observations reported in Sahraoui et al. (2009, 2010a). The presence of a clear break near the electron scales in Figure 3(c) invalidates the argument that the break at electron scales is essentially caused by the foreshock electrons present in the data analyzed in Sahraoui et al. (2009). Indeed, as discussed in Sahraoui & Goldstein (2010), the presence of

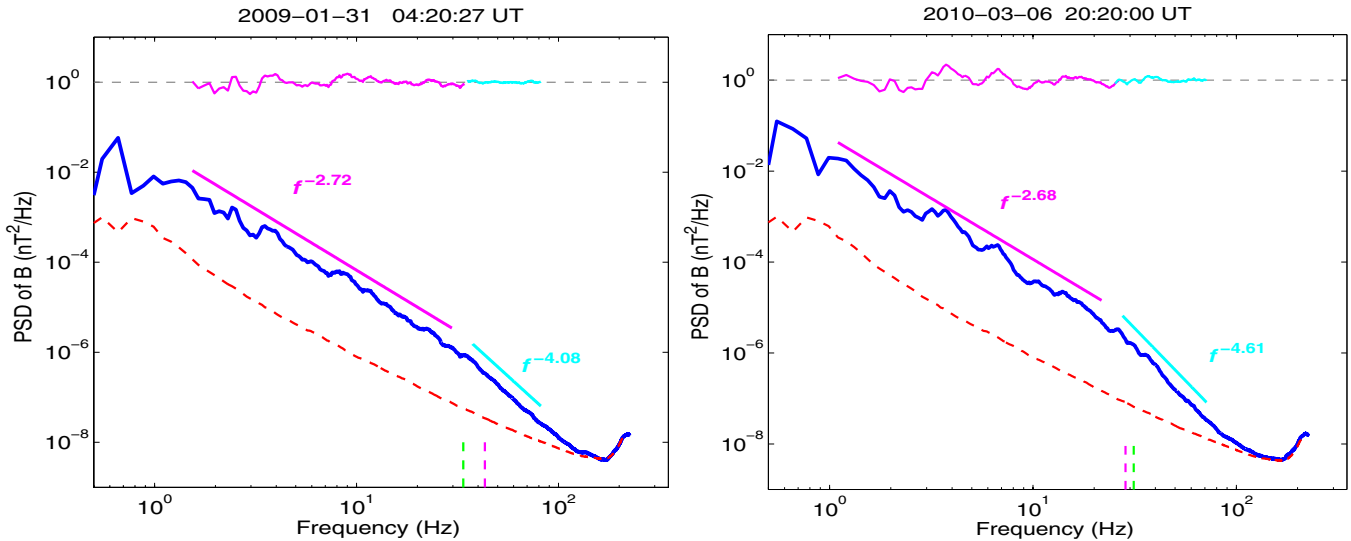


Figure 4. Examples of the magnetic energy spectra measured in the free SW showing a clear spectral break near the Taylor-shifted electron scales f_{de} (green) and f_{pe} (red; vertical dashed lines). The double-power-law model is used to fit the spectra. (A color version of this figure is available in the online journal.)

foreshock electrons may generate a “bump” in the magnetic spectra at that scale, similar to the one shown in Figure 3(a) in Sahraoui et al. (2009), but it is not clear how they could generate a spectral break followed by a steep power-law spectrum as shown in Figure 3(b) of Sahraoui et al. (2009). In any case, the results shown here, which were obtained from SW data that contained no foreshock electrons, clearly prove that the spectral break cannot be attributed to foreshock electrons and most likely results from the nonlinear dynamics of the plasma itself. This indeed has been observed in two-dimensional and three-dimensional PIC simulations (Camporeale & Burgess 2011; Chang et al. 2011; Gary et al. 2012), predicted by existing theories on SW turbulence (Schekochihin et al. 2009; Meyrand & Galtier 2010) and observed also in magnetosheath turbulence (Huang et al. 2013).

A comparison in Figure 3(c) of the computed magnetic energy spectrum with the fitting models discussed in Section 3 shows that the double-power-law model fits the data better as it captures the observed spectral break. The exponential model is shown not to correctly reproduce the scaling in the range $k\rho_e \sim [0.1, 1]$, contrary to the result reported in Alexandrova et al. (2009).⁶ The disagreement with the observations of Alexandrova et al. (2009) can be explained by the lack of universality of turbulence at electron scales, or by the caveats discussed in Section 5. The rapid decay of the exponential model and its failure to fit the spectra in the scale range $\sim [0.1, 1]k\rho_e$ may have been the reason that led to correcting it by a power-law function to sustain the cascade down to $k\rho_e \sim 1$ (Alexandrova et al. 2012), which better reflects SW observations. In that study, it was also shown that 30% (out of 100) of the analyzed STAFF-SA spectra agreed with the double-power-law (or the break) model used here. From Figure 3(c), one can furthermore see that the hybrid and the asymptotic-double-power-law fail to fit the spectral break and the neighboring frequencies, but they reproduce the overall shape of the spectrum, in particular the asymptotic-double-power-law. Nevertheless, these two models

are very close to each other; significant differences appear only at high frequency where the noise floor of the instrument is reached. From this, one concludes that, given that the highest S/N values available from the *Cluster*/SCM data in the SW are at best similar to that of Figure 3, it is unrealistic to expect that one will be able to distinguish between these two models in SW observations. However, the double-power-law model can be distinguished from the two other (curved) models provided that the spectral break can be observed, and, as discussed in Section 5, that requires particular care as such a break is easy to smooth out. For these reasons, we choose to keep only the double-power-law model in our statistical survey to fit the measured magnetic energy spectra.

Among the total 610 spectra (computed over 10 s) found to have $S/N > 10$ at $f = 30$ Hz, 461 (75%) were found to show a break at electron scales. Two other examples of those spectra are plotted in Figure 4. They show very similar features to the spectrum of Figure 3(c). The remaining 25% of the spectra either do not show clear breaks, among them those corresponding to fast SW ($V \gtrsim 800$) where the electron breaks would be shifted to high frequency ($\gtrsim 180$ Hz) and are thus not accessible to the STAFF-SC, or they show bumps at electron scales. These events are disregarded.

The histograms of the obtained slopes are given in Figure 5. We can see that the slopes of the spectra in the dispersive range (i.e., $[f_{\rho_i}, f_{\rho_e}]$) cover the range $\sim [-2.5, -3.1]$ with a peak at ~ -2.8 . These values are close to those predicted by existing theoretical and numerical simulations (Camporeale & Burgess 2011; Chang et al. 2011; Howes et al. 2011b; Boldyrev & Perez 2012) and to the observations reported in Alexandrova et al. (2012). The spectra below f_{ρ_e} are, however, steeper with slopes distributed in the range $\sim [-3.5, -5.5]$ and a peak at ~ -4 , which are in general agreement with the predictions from the two-dimensional and three-dimensional PIC simulations (Camporeale & Burgess 2011; Chang et al. 2011; Gary et al. 2012) and with the results of the break model reported in Alexandrova et al. (2012). This broad distribution suggests the lack of universality of turbulence at electron scales as compared to that in the inertial range. A similar study has been performed on magnetosheath turbulence where

⁶ For the exponential model in Figure 3(c), we fit the frequency range $[0.1, 1]f_b = [2.5, 25]$ Hz, which corresponds to the scale range $k\rho_e \sim [0.08, 0.8]$ with the measured parameters $V_{\text{flow}} \sim 400$ km s⁻¹, $\rho_i \sim 125$ km and $T_i/T_e \sim 2$.

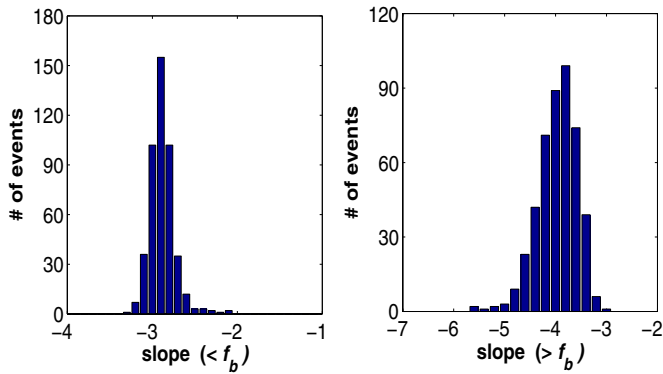


Figure 5. Histograms of the slopes resulting from a double-power-law fits of the scales below (left) and above (right) the frequency f_b corresponding to the spectral break near the electron gyroscale.

(A color version of this figure is available in the online journal.)

steeper spectra above f_{ρ_e} were observed and whose slopes were distributed in the interval $\sim[-4, -7.5]$ with a peak near -5.5 (Huang et al. 2013). We will discuss this point further below.

Another important question that we can try to answer here is the actual physical scale, ρ_e or d_e , that would correspond to the spectral breaks observed within the data. This question relates to the appropriate theoretical description of the electron scales, physics (Schekochihin et al. 2009; Bourouaine et al. 2012). In the so-called Hall-MHD approximation, which is valid in the limit of $\beta_i \ll 1$ and $T_i \ll T_e$ (Schekochihin et al. 2009), the Hall term brings a correction to the classical MHD theory proportional to d_i , the ion inertial length. This theory can be extended to electron scale physics within the incompressible EMHD (Biskamp et al. 1999; Meyrand & Galtier 2010) or the reduced two-fluid-theory (Sahraoui et al. 2003, 2012). Within the EMHD model, which is appropriate for describing whistler mode turbulence, d_e arises as the relevant scale to describe electron scales, physics. However, in the SW at 1AU, where $\beta_i \sim 1$ and $T_i/T_e \gtrsim 1$ (see Figure 2), these popular models are not rigorously valid (Schekochihin et al. 2009; Howes 2009), although they may reproduce some observed properties of SW turbulence such as the scaling of the magnetic or the electric energy spectra in the dispersive range (Matthaeus et al. 2008).

In kinetic theory, recent three-dimensional PIC simulations of electron scales, whistler turbulence showed that a spectral break occurs near d_e (Chang et al. 2011; Gary et al. 2012) and not at ρ_e (note that in Chang et al. 2011 $\beta_e = 0.1$, which means that $\rho_e = d_e/\sqrt{\beta_e} \sim 3d_e$). On the other hand, kinetic theory of KAW turbulence in the limit $k_{\parallel} \ll k_{\perp}$ predicts that the relevant scales are ρ_i and ρ_e . A simple explanation of this can be found from examination of the linear dispersion relations of the KAW at different values of β_i (or β_e) as shown in Figure 6 (top). Regardless of the value of β_i , the KAW becomes dispersive at $k\rho_i \sim 1$ and no significant change is observed at $kd_i \sim 1$.

From an observational point of view, answering the question as to whether ρ_i or d_i is the relevant scale is more difficult because SW data at 1AU often show that $\beta_i \sim 1$, which means that one cannot distinguish the two scales. Nevertheless, some statistical studies have tried to answer this question (Leamon et al. 1999; Bourouaine et al. 2012). For electron scales, only a few studies based on a limited number of events have reported the relevance of ρ_e to characterize electron scale physics in the SW (Sahraoui et al. 2009, 2010a; Alexandrova et al. 2009). Alexandrova et al. (2012) have confirmed that

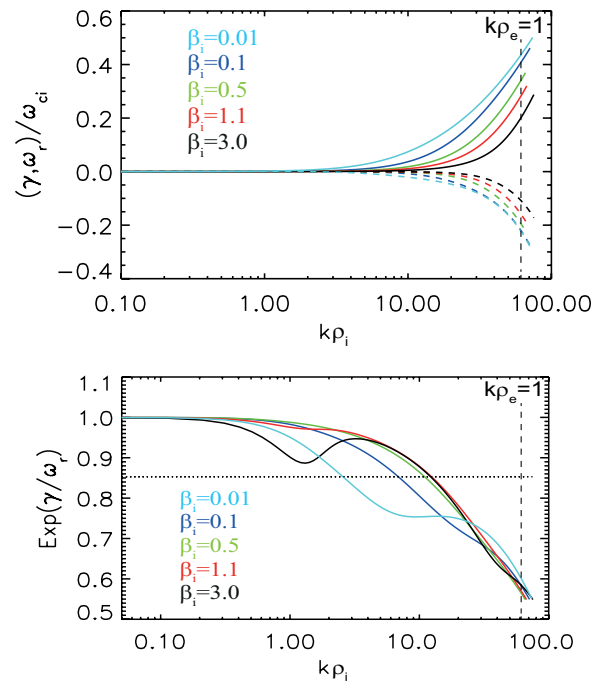


Figure 6. Top: KAWs dispersion relations and damping rates normalized to the proton gyrofrequency for $\theta_{KB} = 89.99$ and the given values of β_i . Bottom: the damping rates of the same modes normalized to one wave period.

(A color version of this figure is available in the online journal.)

result over a larger data samples (100 spectra). In Figure 7, we computed the correlation between the frequencies of the observed spectral breaks with f_{ρ_e} and f_{d_e} . The figure shows a relatively high correlation (0.72) of the spectral break with the electron gyroscale ρ_e than with the inertial length d_e . This result contrasts with the result in Alexandrova et al. (2012) which showed no correlation ($C \sim 0.03$) between the spectral breaks (given by the used double-power-law model) and ρ_e . A possible explanation of the lack of the correlation in that work is the downsampling frequency of the STAFF-SA that does not allow one to properly capture the spectral breaks (see Section 5.2). We note that the moderate correlation with d_e (0.58) may be due to all intervals that have $\beta_e \sim 1$ (for those events $\rho_e \sim d_e$). Finally, we note that a similar correlation coefficient between f_b and ρ_e is found in magnetosheath turbulence (Huang et al. 2013), but a weaker correlation is found with d_e ($C = 0.27$). All of these observations suggest the relevance of ρ_e as a dissipation scale for the SW and the magnetosheath.

5. INSTRUMENTAL CAVEATS AND DATA LIMITATIONS

The results shown in the previous sections were obtained from a 10 yr survey of *Cluster* SCM waveform data in BM. Thus, they provide a reliable statistical image on the scaling of the magnetic energy spectra at electron scales. Nevertheless, these results should be considered within some limitations, related to the instrument itself and to the methods of analyzing the data, which we now discuss in detail.

5.1. Low Amplitude Fluctuations and the Sensitivity of the SCM

The *Cluster* SCM data are so far the only available data allowing one to probe into electron scales of SW turbulence with relatively high S/N. Indeed, current space missions (e.g., *Stereo*, *Wind*, and *THEMIS*) either do not have SCM or do, but with limited sensitivity. The sensitivity

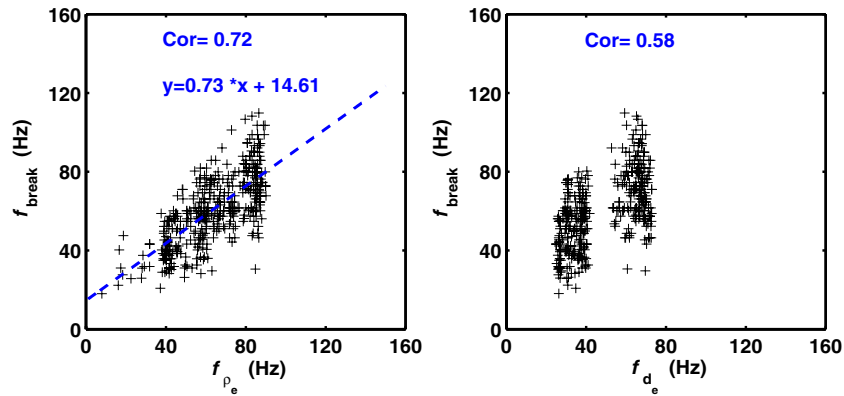


Figure 7. Correlation between the frequencies of the observed spectral breaks f_b with the Taylor-shifted electron gyroscale ρ_e (right) and inertial length d_e (left). (A color version of this figure is available in the online journal.)

of the SCM is essentially (but not exclusively) limited by the length of the magnetic sensor, which is generally constrained by the payload on the spacecraft. For instance, the SCMs onboard *Cluster*, THEMIS, and Magnetospheric Multi Scale (MMS) have sensors with respective lengths of 27 cm, 15 cm, and 10 cm, which yields respective sensitivity levels of 0.4, 0.7, and $2.3 pT/\sqrt{\text{Hz}}$ at 10 Hz.

Despite the relatively high sensitivity of the *Cluster* SCM compared with other space missions, the sensitivity is still not always sufficient for measuring SW magnetic fluctuations above ~ 30 Hz because the amplitudes can be too low (see Figures 7 and 8 in Sahraoui et al. 2010b and Figure 1 in this paper). Indeed, when the measured S/N is exceptionally high (typically $S/N \gtrsim 30$), one should suspect the crossings of boundaries such as IPSs or CMEs (e.g., the event of 2004 January 22 studied in Alexandrova et al. 2009, 2012). We recall that *Cluster*, THEMIS, and MMS are magnetospheric missions and have been designed to essentially address the physics of different regions of Earth’s magnetosphere and the magnetosheath where the magnetic fluctuations generally have higher amplitudes than in the SW (Sahraoui et al. 2004, 2006).

It follows from this discussion that, in order to properly address the problem of energy cascade and dissipation in the SW at frequencies $f_{sc} \gtrsim 30$ Hz, it is important to select SW data when the fluctuations amplitude is very high compared to the sensitivity floor of the *Cluster* SCM. Because of this limited S/N in the SW, Alexandrova et al. (2009) proposed subtracting the sensitivity of the instrument from the measured power spectra. Without discussing in detail the foundation of a such procedure from a signal processing point of view, we can only emphasize the effect that such a procedure has on the scaling of the resulting “denoised” spectra. Indeed, when the S/N becomes very low at a given frequency f_0 , i.e., $\delta B^2(f \gtrsim f_0) = (1 + \epsilon(f))\delta B_{\text{sens}}^2(f \gtrsim f_0)$ with $\epsilon(f) \ll 1$, subtracting the sensitivity of the instrument from the actual spectrum yields a spectrum that falls to zero: $\delta B^2 - \delta B_{\text{sens}}^2 \sim \epsilon \delta B_{\text{sens}}^2$. It is not surprising that, on the log-log scale, such a vanishing spectrum will be seen as exponentially falling-off for all frequencies $f \gtrsim f_0$ (Alexandrova et al. 2009).

5.2. Limited Frequency Resolution of STAFF-Spectrum Analyzer

The STAFF instrument onboard *Cluster* has a single tri-axial SCM, but has two sub-experiments. STAFF-SC measures magnetic field fluctuations (i.e., waveforms) with two possible sampling times, 25 samples s^{-1} (normal mode) and 450 samples s^{-1}

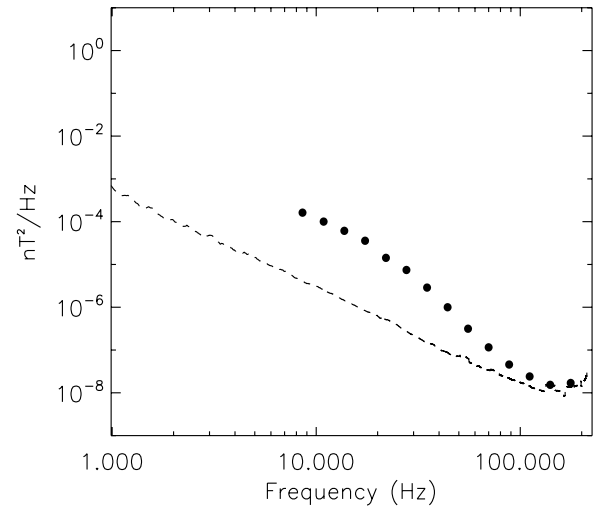


Figure 8. Spectrum of Figure 4 as it would have been measured by STAFF-SA with the available sampling frequencies.

(BM); however, the waveforms are low-pass filtered at 10 Hz and at 180 Hz, respectively (Cornilleau-Wehrin et al. 1997). STAFF-SA computes the 5×5 spectral matrix of the three components of the magnetic field and the two components of the electric field fluctuations (Gustafsson et al. 1997) onboard the spacecraft. STAFF-SA transmits the computed correlation matrix on the central frequencies f_0 of 27 channels logarithmically spaced in the frequency range [8 Hz, 4 kHz] whose bandwidth is proportional to f_0 , $\Delta f = 13\% f_0$. In BM, the interval reduces to approximately [70 Hz, 4 kHz]. It is important to emphasize here that, due to the limited S/N in the SW, which generally does not allow us to address frequencies (in the spacecraft frame) higher than ~ 100 Hz and considering that the Taylor-shifted electron gyroscale is typically $f_{\rho_e} \sim 70$ Hz,⁷ STAFF-SA provides information only at a few frequencies in the interval [8, 100] Hz: $\sim [9, 11, 14, 18, 22, 28, 35, 44, 55, 70, 88]$ Hz. This limited frequency resolution, in the scale range between proton and electron gyroscals, may lead to missing any spectral breaks or not localizing them properly. In both cases, the determination of the scaling of the spectra at electron scales may not be very accurate. To illustrate this problem, in Figure 8 we plotted the same spectrum as in Figure 4 (measured by STAFF-SC) as it

⁷ For SW speed of $\sim 600 \text{ km s}^{-1}$. Faster SW yields higher values of f_{ρ_e} that can be larger than 100 Hz. In this case using STAFF-SA spectra may prove to be useful to study the electron dissipation range forming above f_{ρ_e} .

would have been measured by STAFF-SA. We can see that, while the spectral break can be observed easily in Figure 4 (at $f \sim 30$ Hz), it becomes difficult to identify in Figure 8. The limited number of available points (~ 10) would also make any fit subject to high uncertainties (i.e., large error bars).

This effect may be particularly relevant for explaining the very low correlation ($C = 0.03$) between the spectral breaks and ρ_e reported in Alexandrova et al. (2012) as compared to the one shown in Figure 7 ($C = 0.72$), which is obtained using the STAFF-SC BM waveforms. STAFF-SA is certainly useful for providing information on the overall shape of the spectra at high frequency. However, it may not suffice for addressing specific details such as the actual scaling of the spectra at electron scales. When available, BM STAFF-SC data is certainly the more appropriate data set to use for investigating this problem. The available range of frequencies ($[1, 180]$ Hz) is generally sufficient to determine electron scale physics. In cases when electron scales would correspond to higher frequencies in the spacecraft frame (e.g., fast SW, or quasi-parallel whistler-like fluctuations) not accessible to STAFF-SC, one might use STAFF-SA spectra to probe into electron scales (provided that the S/N remains sufficiently high at those frequencies).

5.3. Time or Frequency Averaging of the Power Spectra

Another effect that may also influence the determination of the scaling of the turbulent spectra at electron scales is the time (or frequency) averaging of the spectra, which is usually done to smooth the spectra under the assumption of time stationarity of the fluctuations. The approach generally consists of dividing a given time series into several shorter intervals of time for which a power spectrum is computed. Then the resulting spectra are averaged to reduce the noise, particularly at high frequencies. However, considering that the turbulent fluctuations are not stationary, averaging the spectra may result in missing some of the information contained in the individual spectra. This is particularly true regarding the presence of a spectral break at electron scales. For instance, let us assume that each given subinterval of time yields a power spectrum with a clear breakpoint at a given frequency f_b in the spacecraft reference frame. If the value of the frequency f_b changes from one subinterval of time to the other, due to small scale physics or fluctuations either in the mean SW parameters (e.g., V_{sw} , T_i , T_e , V_A) that enter in estimating the scale ρ_e or the corresponding frequency f_{ρ_e} , and if the individual spectra have comparable power, then averaging them will result in smoothing the spectral breaks, yielding a curved spectrum in the frequency range corresponding to all of the breaks. To show this, we have plotted three spectra computed over 10 s within a window of 10mn in Figure 9 (top panel). The three spectra show clear breakpoints at approximately 20 Hz, 30 Hz, and 45 Hz. When the three spectra were averaged (bottom panel), they yielded a spectrum without any clear break in the frequency range $[20, 45]$ Hz. The spectrum curves at those frequencies and can be well fit by exponential-like models.

5.4. Instrumental Interference at High Frequency

The last instrumental problem that can affect the proper determination of the scaling of the magnetic energy spectra in the SW is the presence of interference observed at high frequency of STAFF-SC spectra. Examples of such interference are shown in Figure 10.

Although the spikes caused by such interference are few, their relatively high amplitudes may nevertheless affect the fit of the

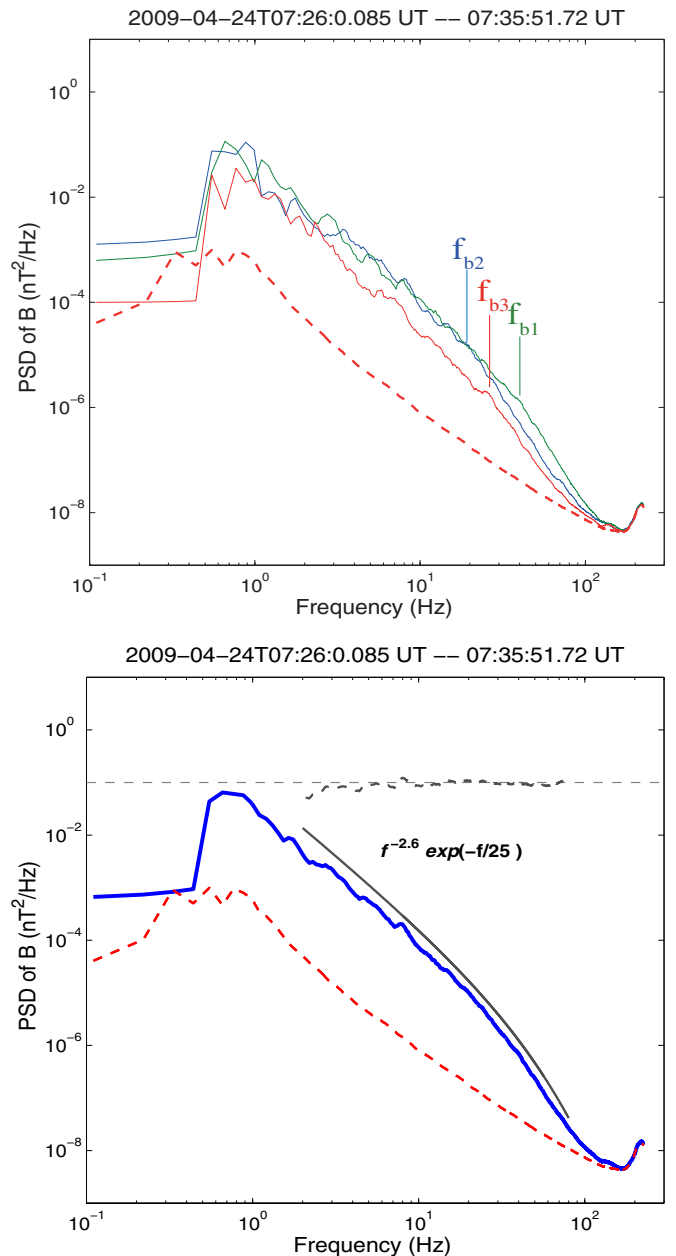


Figure 9. Three magnetic energy spectra measured in the SW (computed over 10 s each) showing breakpoints at different frequencies indicated by the vertical lines (top). The mean spectrum shows no clear break and curves at those frequencies (bottom). The horizontal curve (bottom panel) shows the compensated spectrum $B^2(f)/P(f)$ where $P(f)$ is the used fitting function. The dashed line is the sensitivity floor of the *Cluster* SCM.

(A color version of this figure is available in the online journal.)

turbulent spectra at electron scales. Indeed, when smoothed, the intense spikes lead to overestimating the power at the highest part of the spectra, which then produces shallower spectra as shown in Figure 10 (top). The figure compares smoothing by a mean and median function on windows of size, logarithmically increasing with frequency. The effect of interference becomes more important for spectra with low S/N, which emphasizes the need to use the highest available S/N in the SW.

From Figure 10, we can also see that the four *Cluster* satellites are not affected equally by the interference. A more complete study (not shown here) revealed that C1, and particularly its B_z component, is most affected. Therefore, considering that most

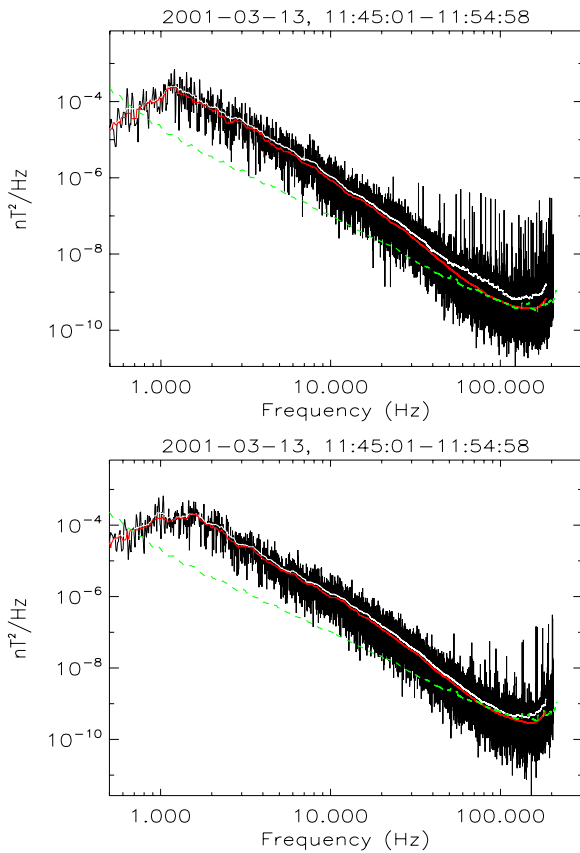


Figure 10. Example of high frequency spikes (interferences) observed on the spectra of B_z (GSE) measured by the STAFF instrument on C1 (top) and C2 (bottom). The corresponding smoothed spectra mean (white) and median (red) functions are shown. The dashed green line is the in-flight mean sensitivity floor of STAFF.

(A color version of this figure is available in the online journal.)

of the studies of the electron scales in the SW are based on single spacecraft data, one should use data from C2, C3, or C4. Depending on the level of the S/N, the number and amplitude of the spikes that appear on the spectra, it might be necessary to pre-process the data prior to analysis in order to reduce the effect of those spikes.

Finally, we note that this interference would also affect the spectra computed by the STAFF-SA instrument onboard the spacecraft. Owing to the fact that the STAFF-SA spectra are averaged over a frequency band centered at each of the 27 frequencies, the contribution of the spikes is very likely to be included in the transmitted energy density. Because the original waveforms are lost, it is not possible to quantify the effect of the interference on the STAFF-SA spectra.

6. DISCUSSION

The results shown in the previous sections underline the need to carefully handle the *Cluster*/STAFF data in the SW in order to properly analyze the energy spectra at electron scales. We have shown that in order to reveal the presence of spectral breaks at electron scales, data intervals with high S/N are required. For the selected data, about 75% of the total number of magnetic energy spectra was found to have a spectral break near the electron scale, followed by steep power-law-like spectra f^α . The distribution of their slopes, α , was shown to range from -3.5 to -5.5 with a peak near -4 . This distribution is broader than that of the slopes in the dispersive range,

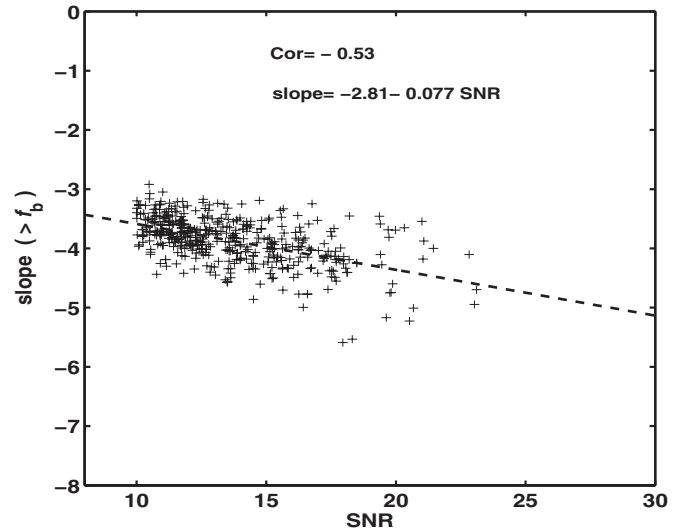


Figure 11. Correlation between the frequencies of the observed spectral breaks f_b with the S/N (see the text) at 30 Hz of the studied magnetic energy spectra.

which covers the values $-3.2 \lesssim \alpha \lesssim -2.3$. A comparison of these distributions with those reported for magnetosheath turbulence (Huang et al. 2013) shows some interesting similarities and differences. In the dispersive range, the distribution of the slopes is very similar: both are narrow and show a peak near -2.8 , in general agreement with most of the theoretical and numerical predictions on SW turbulence. However, in the electron dissipation range, the magnetosheath spectra were generally steeper with slopes as low as $\alpha \sim -7$, whose distribution peaks near -5.5 . This comparison stimulated a further analysis of the data to explain the difference between the SW and magnetosheath observations based on the differences in the S/Ns between the two regions. Let us examine this effect.

Although the data used here have the highest found S/N in more than 10 yr of data survey in the SW, it might be possible that even S/N values as high as 10 are insufficient for accurately determining the scaling above f_b . This is a result of the limited extension of the spectrum above f_b (typically less than one decade) due to the proximity of the sensitivity floor of the SCM. To test this hypothesis, we plotted in Figure 11 the measured slopes of the spectra above f_{pe} as a function of the corresponding S/N in Figure 11. The figure shows a moderate correlation ($C = 0.53$) between the S/N and the slopes. Typically, most of the slopes $|\alpha| \lesssim 3.5$, which were not observed in magnetosheath turbulence, correspond to $S/N < 15$, and the highest values of the slopes $|\alpha| \gtrsim 4.5$ correspond to $S/N \gtrsim 15$. This correlation suggests that data with even higher S/N are needed to fully address the actual scaling of the magnetic energy spectra at sub-electron scales in the SW. Based on this conclusion, the power-law fits and the interpretation of the low values of slopes ($|\alpha| \lesssim 3.5$) reported in this study should be considered with some caution. We emphasize that a weak correlation ($C < 0.1$) is found in magnetosheath turbulence when $S/N > 25$ (Huang et al. 2013).

Another interesting point to discuss is the possible dependence of the scaling of the magnetic energy spectra in the dispersive and dissipation ranges on the plasma β_i . If one assumes that turbulence below the ion scale is dominated essentially by highly oblique KAWs, as suggested by several SW observations (Bale et al. 2005; Sahraoui et al. 2009, 2010a; Salem et al. 2012;

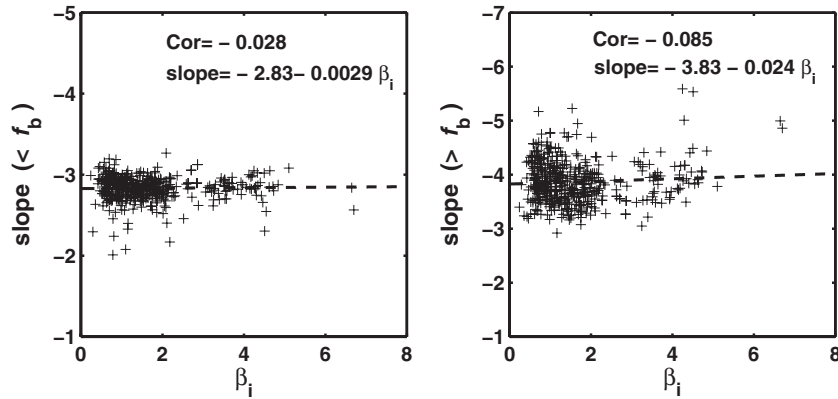


Figure 12. Correlation between the frequencies of the observed spectral breaks f_b with the plasma β_i of all analyzed time intervals below (left) and above (right) the spectral break.

Podesta & Tenbarge 2012; Kiyani et al. 2013; Chen et al. 2013), such a dependence could exist. This is based on the known result from the linear kinetic theory that the damping of high oblique KAWs depends strongly on the plasma β_i . This can be seen clearly in Figure 6 (top panel) which shows that the lower the β_i is, the more damped the KAW mode is (for the same angle of propagation). Based on this, one would expect to observe a rapid decay of the energy spectra at low β_i , which would translate into steeper power-law or exponentially decaying spectra (Howes et al. 2011a). To test this, we plotted the correlation between the observed slopes below and above f_{pe} as a function of β_i in Figure 12. The results do not show any clear dependence between the values of the slopes and β_i . A possible explanation is that the difference in the kinetic damping of the KAW modes is more pronounced between $\beta_i \sim 1$ and much lower values, $\beta_i \sim 0.01$. This cannot be seen directly in Figure 6 (top). Figure 6 (bottom) shows the damping of each KAW mode over one wave period as evidence. The figure shows that the modes with $\beta_i \gtrsim 0.5$ have nearly the same normalized damping rate at all scales, which is very different from the damping of the modes at $\beta_i = 0.01$ and $\beta_i = 0.1$. The latter are shown to undergo strong damping (defined when $2\pi\gamma/\omega_r \sim 1$) at $k\rho_i \sim 3$ and $k\rho_i \sim 10$, respectively. This may explain the absence of a correlation between the slopes and β_i reported in Figure 12, since most of the observations reported here have $\beta_i \gtrsim 0.5$ (see Figure 2). Larger samples of SW data would allow one to obtain lower values of β_i and test the scenario proposed here. Other explanations are also possible, such as the presence of non-local effects (due to large scale shear flows) that would overcome the strong damping at low β_i and sustain the cascade down to the electron scales as suggested in Howes et al. (2011a). Another possibility is that the KAW scenario discussed here may be irrelevant to the present observations. In any case, the origin of the large spread of the slopes above f_{pe} reported here and in magnetosheath turbulence (Huang et al. 2013), as compared to those in the dispersive range, remains unclear and suggests the lack of universality of the turbulence at these small scales. The scaling of the spectra at sub-electron scales may depend on local electron plasma instabilities. Such dependence was indeed found between the slopes of the spectra at sub-ion scales and the local ion plasma instabilities (Bale et al. 2009). Proving the existence of the same dependence at sub-electron scales requires high time resolution measurements (a few milliseconds) of electron distribution functions. Such measurements are not available with the current space missions.

The NASA/MMS mission is expected to meet part of these requirements.

7. CONCLUSIONS

We have surveyed more than 10 yr of the *Cluster* BM SCM data in the SW and focused on the magnetic energy spectra below the ion gyroscale, ρ_i . We discussed several instrumental caveats that may potentially influence the estimation of the scaling of the spectra at electron scales. We showed, in particular, that high S/Ns are needed to properly determine the scaling of the energy spectra. Once all of the caveats were considered, we found a large number of spectra having clear spectral breaks near the Taylor-shifted electron gyroscale, f_{pe} . A double-power-law model has been adopted to fit the spectra. The distribution of the slopes below the spectral break f_b was found to be narrow and centered around ~ -2.8 , while that above the f_b was found to be broader and centered near the value ~ -4 . The peak of the distribution of the slopes below f_b is consistent with similar observations of SW and magnetosheath turbulence (Alexandrova et al. 2012; Huang et al. 2013) and with most of the existing theoretical or numerical predictions. The spectra above f_b are, however, shallower than those reported in magnetosheath turbulence. A possible explanation of that discrepancy is the difference in the S/N between the SW and the magnetosheath. A moderate correlation was indeed found between small values of the slopes, typically $|\alpha| < 4$, with lower values of S/N. The reported wide distribution of the slopes combined with earlier observations that showed exponential-like scaling indicate that the physics of the electron scales is possibly not universal and might be controlled by several plasma parameters. A firm conclusion as to which fitting model is dominant in the SW remains to be elucidated with the future space mission that will provide magnetic field data with higher S/N. Based on the assumption that KAW turbulence dominates at electron scales and on the fact that the linear damping of the KAW modes (from the Vlasov–Maxwell equations) strongly depends on β_i , an attempt to find a correlation between the observed slopes and the plasma β_i was carried-out, but the result was not conclusive.

The *Cluster*-search coil data allow for unprecedented in-depth studies of electron scale turbulence in the SW. However, as shown in this study, magnetic field data with higher S/N is now needed to fully and unambiguously characterize the turbulence cascade and dissipation at electron scales in the SW. Furthermore, one needs to have accurate measurements

of electric field fluctuations and high time resolution of ion and electron distribution functions, which are not available on current space missions. A new mission, TOR, is currently being designed to fulfill these requirements.

This work is part of the project THESOW funded by L'Agence Nationale de la Recherche (ANR, France). J. De Patoul is funded through the ANR grant. The FGM, CIS, and PEACE data come from the CAA (ESA) and AMDA (CDPP, IRAP, France). FS thanks O. Gurcan and N. Cornilleau-Wehrlin for fruitful discussions and P. Canu for providing the WHISPER data.

REFERENCES

- Alexandrova, O., Lacombe, C., Mangeney, A., Grappin, R., & Maksimovic, M. 2012, *ApJ*, **760**, 121
- Alexandrova, O., Saur, J., Lacombe, C., et al. 2009, *PhRvL*, **103**, 165003
- Bale, S. D., Kasper, J. C., Howes, G. G., et al. 2009, *PhRvL*, **103**, 211101
- Bale, S. D., Kellogg, P. J., Mozer, F. S., Horbury, T. S., & Rème, H. 2005, *PhRvL*, **94**, 215002
- Biskamp, D., Schwarz, E., Zeiler, A., Celani, A., & Drake, J. F. 1999, *PhPl*, **6**, 751
- Boldyrev, S., & Perez, J. C. 2012, *ApJL*, **758**, L44
- Bourouaine, S., Alexandrova, O., Marsch, E., & Maksimovic, M. 2012, *ApJ*, **749**, 102
- Camporeale, E., & Burgess, D. 2011, *ApJ*, **730**, 114
- Chang, O., Gary, S. P., & Wang, J. 2011, *GeoRL*, **38**, L22102
- Chen, C. H. K., Boldyrev, S., Xia, Q., & Perez, J. C. 2013, *PhRvL*, **110**, 225002
- Cornilleau-Wehrlin, N., Chauveau, P., Louis, S., et al. 1997, *SSRv*, **79**, 107
- Décréau, P., Ferreau, P., Krannosels'kikh, V., et al. 1997, *SSRv*, **79**, 157
- Gary, S. P., Chang, O., & Wang, J. 2012, *ApJ*, **755**, 142
- Gurcan, O. D., Garbet, X., Hennequin, P., et al. 2009, *PhRvL*, **102**, 255002
- Gustafsson, G., Bostrom, R., Holback, B., et al. 1997, *SSRv*, **79**, 137
- Hasegawa, A., Imamura, T., Mima, K., & Taniuti, T. 1978, *JPSJ*, **43**, 255002
- Howes, G. 2009, *NPGeo*, **16**, 219
- Howes, G., TenBarge, J. M., & Dorland, W. 2011a, *PhPl*, **18**, 102305
- Howes, G., TenBarge, J. M., Dorland, W., et al. 2011b, *PhRvL*, **107**, 035004
- Huang, S. Y., Sahraoui, F., Deng, X. H., et al. 2013, *PRL*, submitted
- Johnstone, A. D., Alsop, C., Burge, S., et al. 1997, *SSRv*, **79**, 351
- Kiyani, K. H., Chapman, C., Khotyaintsev, Yu. V., Dunlop, M. W., & Sahraoui, F. 2009, *PhRvL*, **103**, 075006
- Kiyani, K. H., Chapman, C., Sahraoui, F., et al. 2013, *ApJ*, **763**, 10
- Leamon, R. J., Smith, C. W., & Ness, N. F. 1999, *JGR*, **104**, 22331
- Matthaeus, W. H., Servidio, S., & Dmitruk, P. 2008, *PhRvL*, **101**, 149501
- Meyrand, R., & Galtier, S. 2010, *ApJ*, **721**, 1421
- Meyrand, R., & Galtier, S. 2012, *PhRvL*, **109**, 194501
- Podesta, J. J., Borovsky, J. E., & Gary, S. P. 2010, *ApJ*, **712**, 685
- Podesta, J. J., & TenBarge, J. M. 2012, *JGR*, **117**, A10106
- Rème, H., Aoustin, C., Bosqued, J. M., et al. 2001, *AnGeo*, **19**, 1303
- Sahraoui, F., Belmont, G., & Goldstein, M. L. 2012, *ApJ*, **748**, 100
- Sahraoui, F., Belmont, G., Pinçon, J., et al. 2004, *AnGeo*, **22**, 2283
- Sahraoui, F., Belmont, G., & Rezeau, L. 2003, *PhPl*, **10**, 1325
- Sahraoui, F., Belmont, G., Rezeau, L., et al. 2006, *PhRvL*, **96**, 075002
- Sahraoui, F., & Goldstein, M. L. 2010, in *AIP Conf. Ser.* 1320, *Modern Challenges in Nonlinear Plasma Physics*, ed. D. Vassiliadis, S. F. Fung, X. Shao, I. A. Daglis, & J. D. Huba (Melville, NY: AIP)
- Sahraoui, F., Goldstein, M. L., Belmont, G., Canu, P., & Rezeau, L. 2010a, *PhRvL*, **105**, 131101
- Sahraoui, F., Goldstein, M. L., Belmont, G., et al. 2010b, *P&SS*, **59**, 585
- Sahraoui, F., Goldstein, M. L., Robert, P., & Khotyaintsev, Y. V. 2009, *PhRvL*, **102**, 231102
- Salem, C. S., Howes, G. G., Sundkvist, D., et al. 2012, *ApJL*, **745**, L9
- Schekochihin, A., Cowley, S. C., Dorland, W., et al. 2009, *ApJS*, **182**, 310
- Valentini, F., Califano, F., Perrone, D., Pegorano, F., & Veltri, P. 2011, *PhRvL*, **106**, 165002